ISBN: 978-3-95450-179-3 doi:10.18429/JACoW-FEL2017-MOP013

HUNDRED-GIGAWATT X-RAY SELF-SEEDED HIGH-GAIN HARMONIC GENERATION

L. Zeng[#] , S. Zhao, W. Qin, S. Huang, K. Liu
Institute of Heavy Ion Physics, School of Physics, Peking University, Beijing 100871, China
Y. Ding , Z. Huang
SLAC National Accelerator Laboratory, Menlo Park, CA 94025, USA

Abstract

Self-seeded high-gain harmonic generation is a possible way to extend the wavelength of a soft x-ray free-electron laser (FEL). We have carried out simulation study on harmonic generation within the photon energy range from 2 keV to 4.5 keV, which is difficult to be achieved due to a lack of monochromator materials. In this work we demonstrate the third harmonic FEL with the fundamental wavelength at 1.52 nm. Our result shows that, by using undulator tapering technique, hundred-gigawatt narrow-bandwidth FEL output can be obtained.

[*]INTRODUCTION

Free-electron lasers, the so called fourth generation of light source, allow one to carry out completely new experiments in atomic and molecular physics, chemistry and many other areas. Self-amplified spontaneous emission (SASE) [1,2] is the baseline FEL operation mode in X-ray region, which has good transverse coherence. However, it starts from the shot noise of the electron beam, which leads to the poor properties in terms of a spectral bandwidth.

Several external seeding FEL schemes are proposed to obtain good longitudinal coherence. For example, directly HHG[3], HGHG[4,5], cascade HGHG[6], EEHG[7,8] and so on. Because of lacking external seeds with short wavelength, these external seeding FEL schemes have difficulty in demonstrating at hard X-ray region.

Self-seeding [9] is a way to narrow the SASE bandwidth of XFELs significantly in order to produce nearly transform-limited pulses. Last several years, self-seeding scheme has been demonstrated in both soft and hard x-ray FELs [10,11]. The monochoromator for soft x-ray self-seeding FEL (the photon energy below 2 keV) is a grating-based optic system[10]， while the hard x-ray self-seeding FEL (the photon energy above 4.5 keV) usually uses diamond-based monochromator[11]. However, the self-seeded FEL has not been demonstrated in the energy region between 2 to 4.5 keV. Previous study in self-seeded HGHG FEL scheme [12] can not only fill the above energy gap, but also extend the wavelength in hard X-ray self-seeding FEL. Ultra-high power FELs are more attractive for the science application like nonlinear Compton scattering[13]. In this paper, the self-seeded HGHG FEL scheme is further studied to obtain ultra-high peak power.

THE SCHEME

The schematic of the self-seeded HGHG FEL is shown in Fig. 1. At first, the electron beam goes through the undulator U_S, generating SASE radiation in the linear regime. At the exit of U_S, the SASE radiation passes through the grating-based X-ray monochromator so as to obtain a narrow-band seed for the following undulator while the electron beam goes through a bypass chicane C_{B1}. The bypass chicane C_{B1} can not only provides a proper delay to make the electron beam and the seed recombine at the entrance of undulator U_A but also help to wash out the microbunching of the electron beam built up in the SASE undulator. Then, we should notice that this seed is different to external seed of regular HGHG FEL[6]. This seed radiation from the monochromator has a much lower power, limited to a few hundred kilowatts herein because of avoiding damaging the state-of-the-art X-ray monochromator optics. As a result, we need to amplify the seed radiation. At the same time, we have to eliminate the impact of electron energy spread degradation in the seed amplification process. Consequently, an electron beam with longer bunch length is used to generate double-spike seed after monochromator. The head spike of the seed is then aligned with the tail part of the electron bunch at the entrance of the amplifying undulator U_A. Therefore only the tail part of the electron bunch is used to amplify the seed while the head part is kept undisturbed and “fresh”. After the U_A undulator, the electron bunch is delayed by a small chicane (C_{B2}), and consequently the head part is aligned with the seed radiation in the modulation undulator (U_{M2}) and gets energy-modulated. The energy modulated electron beam then goes through the dispersion chicane with proper R_{56}, getting density modulated, and radiates at the harmonic wavelength of the seed.

Compared to previous work in 2016[12], we have finished further study in this paper. (1) Further optimization in the amplifier (U_A), modulator (U_{M2}) and dispersion section (C_D), (2) Tapered radiator (U_R) study for higher output harmonic radiation FEL power. The details in both two parts will be shown in the following section.

#zengling@pku.edu.cn

ISBN: 978-3-95450-179-3 doi:10.18429/JACoW-FEL2017-MOP013

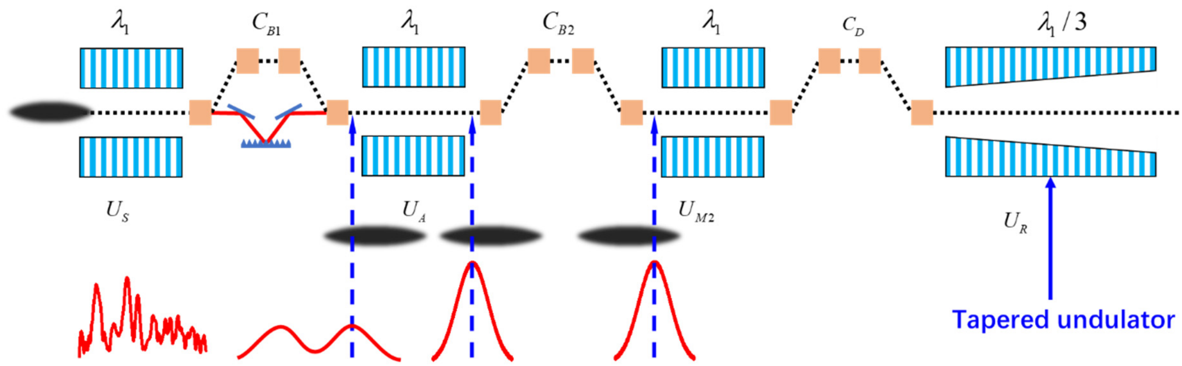

Figure 1: Schematic of tapered self-seeded HGHG FEL. U_S is a SASE undulator, U_A is a seed amplifier, U_{M2} is a modulation undulator, and U_R is a radiation undulator (radiator) of HGHG. C_{B1} and $C_{B2}$are bypass chicanes, while C_D is a dispersion chicane of HGHG.

FEL SIMULATION

Table 1: Parameters used for Self-seeded HGHG Simulation

Parameter	Value	Unit
Electron beam		
Energy	4.3	GeV
Peak current	2.5	kA
Energy spread	1.0	MeV
Emittance	0.5	mm-mrad
Mono / Chicane		
Resolving power	5000	
Power efficiency	0.02	
central wavelength	1.52	nm
Undulators		
undulator period	0.03	m
U_S length	19.8	m
U_S strength, a_u	2.4749	
U_{M2} strength, a_u	2.4749	
U_R strength, a_u	1.6	

Here we use the parameters of the soft X-ray self-seeding (SXRSS) FEL at LCLS for start-to-end simulations. The simulations were performed with GENESIS [14] and the parameters are shown in Table 1. Fig. 2 shows the time-dependent simulation result of radiation after monochromator. A seed with narrow bandwidth is produced for the next HGHG stage. We should notice that the seed power is about 200 kW, which is much lower than that of regular HGHG external seed.

In the amplification section, when a short undulator U_A is used, the seed could not get enough amplified. On the contrary, a long undulator U_A may obtain high seed power, but the “fresh”part of the electron bunch also may be disturbed because of the SASE process itself. Here we made optimization on the length of U_A. The evolution of the seed laser pulse and electron beam in U_A is illustrated in Fig. 3. It is clear from that, while the peak power of the radiation is amplified to about 100 MW in the U_A undulator, the head electrons in the bunch do not get disturbed and the energy spread of the tail electrons becomes larger. After the U_A undulator, the electron bunch is delayed by the C_{B2} chicane, and the head part electrons are aligned with the seed radiation in the U_{M2} modulation undulator.

The remained part is a regular HGHG configuration. The fresh part of the electron bunch is energy modulated by the amplified seed laser at U_{M2}. Enough energy modulation is necessary for nth harmonic. However, we should avoid too much extra energy spread caused by the energy modulation process. The optimized length of U_{M2} is 8 m. Choosing R_{56} =0.42 μm , density modulation is obtained after dispersion chicane C_D . Finally, the 3rd harmonic is generated in the radiator U_R.

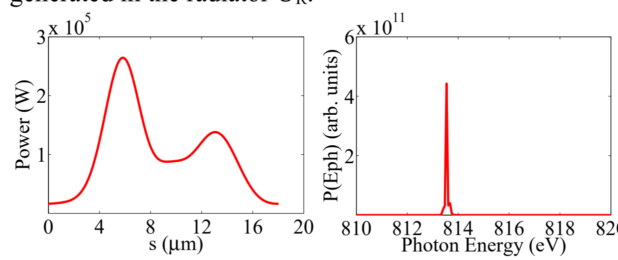

Figure 2: FEL power profile (left) and spectra (right) at the exit of monochromator C_{B1}.

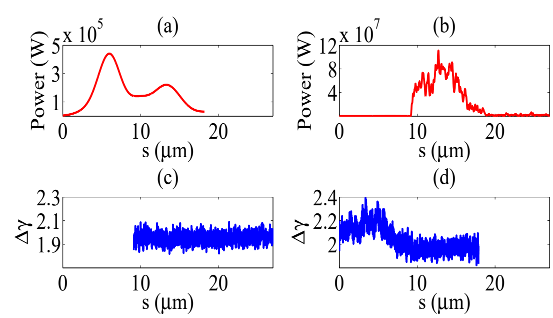

Figure 3: Simulated radiation power (top) and electron beam (bottom) evolution at the entrance to U_A (left), at and at the entrance to U_{M2} (right).

The resonance condition on the central axis of a FEL is given by the equation

$$\lambda_R = \frac{\lambda_u}{2\gamma^2}(1 + a_u^2) \tag{1}$$

ISBN: 978-3-95450-179-3 doi:10.18429/JACoW-FEL2017-MOP013

For regular undulator U_R, the rms undulator parameter a_u is constant. As the FEL power of the radiation grows, the electron beam energy γ drops. Gradually, when the resonance condition can't be maintained, the FEL power reaches saturation. This severely limits the energy extraction efficiency of the FEL. When using tapered undulator U_R, a_u is a function of the axial position z so as to maintain the resonance condition continually as the electrons decelerate. The key problem is finding the proper function $a_u(z)$ or K(z), the so called taper profile.

We analyse two kinds of taper profile of the radiator U_R. Fig.4 shows the common linear taper profile, z_0 is the position where the taper starts, the taper ratio is $k = (\Delta K)/K_0$. From Fig.4, the period in zigzag taper profile is z_T, and defined $\eta_{zig} = \delta K/\Delta K$. From KMR model[15] about tapered undulator, if we want more energy extraction from electron beam, two conditions are necessary. (1), make ponderomotive bucket deceleration rapid. (2), more particles should be trapped by the ponderomotive bucket. However, there is a conflict between rapid bucket deceleration and maintaining a large number of trapped particles[15]. Eventually, different kinds of taper profile have their own advantages and disadvantages. Moreover, for a given type of taper profile, we also need to optimize its key parameters. For linear taper profile, the optimized simulation parameters are: $z_0 = 13.2$ m, k=5%; For zigzag taper profile, the optimized simulation parameters are: $z_0 = 13.2$ m, $z_T = 3.3$ m, k=0.3%, $\eta_{zig} = 50\%$. Fig.7 demonstrates the FEL power evolution in different kinds of undulator. It's clear that by tapering, the FEL power of 3rd harmonic is enhance by about an order of magnitude. The saturation power of linear taper (65GW) is lower than that of zigzag power (75GW). The most possible reason is that the ponderomotive bucket of zigzag taper can trapped some particles which are untrapped before when the bucket moving up.

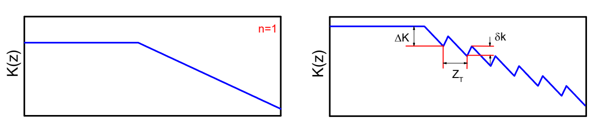

Figure 4: schematic of the linear taper profile (left) and zigzag taper profile (right) undulator

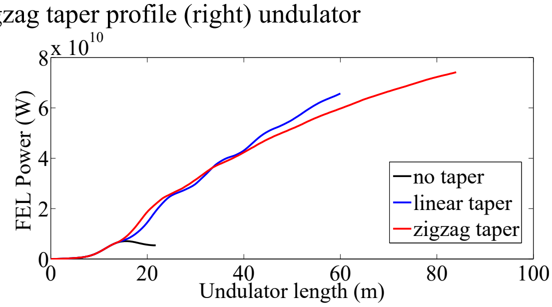

Figure 5: FEL power evolution in different kind of undulator

We have studied linear taper profile above. In addition, nonlinear taper is also important. As we know, the taper law for nonlinear taper profile can be written as

$$K(z) = \begin{cases} K_0 & (0 < z < z_1) \\ K_0 \times \left(1 - k\dfrac{(z-z_0)^n}{{L_t}^n}\right) & (z < z_1) \end{cases}$$

Here L_t is the taper length. We optimize the taper index n of normal taper profile to maximize the saturation power of the self-seeded HGHG FEL. Fig.5 shows the FEL power versus n at the exit of radiator U_R. It demonstrates that when n=1.9, the maximum FEL power of the 3rd harmonic is 155 GW. Fig 7 and Fig 8 demonstrate the power profile and spectra at the exit of U_R. It's obvious that a narrow-bandwidth radiation at hundred-gigawatt level is obtained.

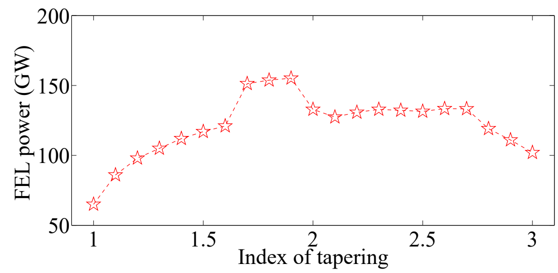

Figure 6: FEL power versus index of tapering in U_R

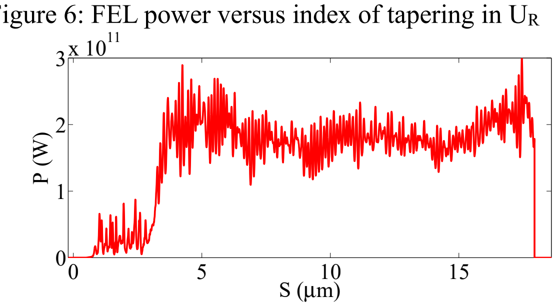

Figure 7: FEL power profile at the exit of U_R (n=1.9)

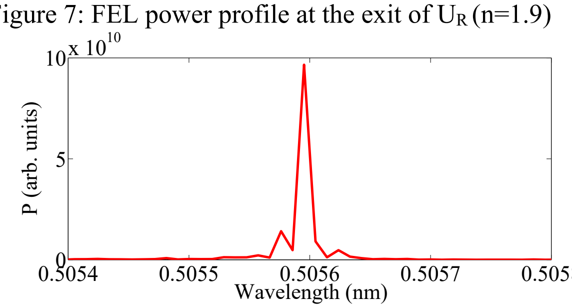

Figure 8: spectrum at the exit of U_R (n=1.9)

CONCLUSION

We proposed a high-peak-power self-seeded HGHG scheme, which is a promising way to extend regular self-seeded FELs to shorter wavelengths, especially within the photon energy range from 2 keV to 4.5 keV, which is difficult to achieve due to a lack of monochromator materials. The simulation result shows that hundred-gigawatt 3rd harmonic radiation (0.5 nm) is obtained by optimizing tapered undulator U_R.

REFERENCES

[1] A. M. Kondratenko and E. L. Saldin, *Part. Accel*, vol. 10, pp. 207-216, 1980.

ISBN: 978-3-95450-179-3 doi:10.18429/JACoW-FEL2017-MOP013

[2] R. Bonifacio, C. Pellegrini, and L. M. Narducci, *Optics Communications*, vol. 50, pp. 373-378, 1984.

[3] G. Lambert *et al.*, *Nature Phys.*, vol. 4, pp. 296-300, 2008.

[4] I. Ben-Zvi *et al.*, *Nucl. Instrum. Methods Phys. Res.*, Sect. A 304, pp. 181, 1991.

[5] L. Yu, *Phys. Rev. A*, vol. 44, pp. 5178, 1991.

[6] J. Wu and L. Yu, *Nucl. Instrum. Methods. A*, vol. 475, pp. 104-111, 2001.

[7] D. Xiang and G. Stupakov, "Echo-enabled harmonic generation free-electron laser", *Phys. Rev. ST. Accel. Beams*, vol. 12, pp. 030702, 2009.

[8] M. Dunning *et al.*, A proof-of-principle echo-enabled harmonic generation FEL experiment at SLAC, Conf. Proc. 2010, C100523 (IPAC-2010-TUPE069)

[9] J. Feldhaus *et al.*, *Optics Communications*, vol. 140, pp. 341-352, Aug. 1997.

[10] D. Ratner *et al., Phys. Rev. Lett*, vol. 114, pp. 054801, 2015.

[11] J. Amann *et al.*, *Nature Photonics*, vol. 6, pp. 693-698, 2012.

[12] L. Zeng, *et al.*, *Chin. Phys. C.* vol. 40, pp. 098102, 2007.

[13] M. Fuchs *et al.*, « Anomalous nonlinear x-ray compton scattering », *Nat. Phys*. Vol. 11, pp. 964, 2015.

[14] S. Reiche, *Nucl. Instrum. Methods A*, vol. 429, pp. 243 1999.

[15] N. M. Kroll, P. L. Morton, and M. Rosenbluth, *IEEE J.Quantum Electron*., vol. 17, pp. 1436, 1981.